Science of the Total Environment 866 (2023) 161114

Contents lists available at ScienceDirect

Science of the Total Environment

journal homepage: www.elsevier.com/locate/scitotenv

# Effects of offshore wind farms on suspended particulate matter derived from satellite remote sensing

I.L.S. Brandao [a,*], J. van der Molen [b], D. van der Wal [a,c]

[a] NIOZ Royal Netherlands Institute for Sea Research, Dept of Estuarine and Delta Systems, P.O. Box 140, 4400 AC Yerseke, the Netherlands
[b] NIOZ Royal Netherlands Institute for Sea Research, Dept of Coastal Systems, P.O. Box 59, 1790 AB Den Burg, Texel, the Netherlands
[c] Faculty of Geo-Information Science and Earth Observation (ITC), University of Twente, P.O. Box 217, 7500 AE Enschede, the Netherlands

## HIGHLIGHTS

- Suspended particulate matter (SPM) is expected to increase in wind farm areas.
- A BACI design was performed to assess changes in SPM around wind farms.
- Scatterplots were used to identify variables influencing SPM around wind farms.
- SPM reduced in impact and control sites and season shaped environmental variables.
- SPM is biased by sampling under clear-sky and optimum meteorological conditions.

## GRAPHICAL ABSTRACT

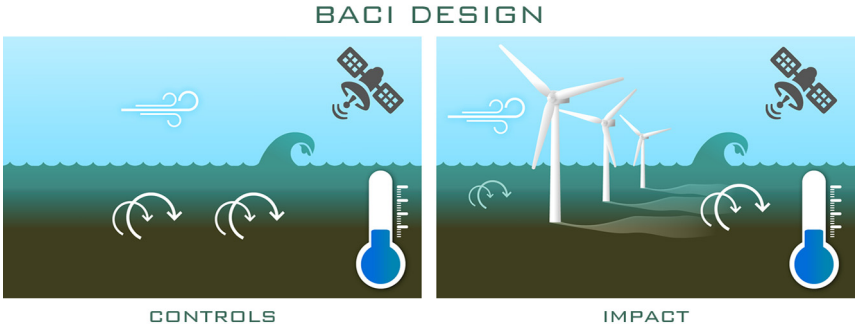


## ARTICLE INFO

Editor: José Virgílio Cruz

## 1. Introduction

Wind energy, as an alternative to fossil fuels, has been considered one of the foremost significant greenhouse gas (GHG) emission reduction measures across the globe since the late 1970s (Swart et al., 2009; Wiser et al., 2011). It has the potential to reduce GHG emissions by over 0.2 Gt $CO_2$/year (GWE C, 2010); therefore, it is essential to achieving goals to limit global warming (IPCC, 2022; UNFCCC, 2015). Alongside their potential benefits for the marine ecosystem (e.g., functioning as artificial reefs, hence resulting in increased species diversity, e.g. of benthic assemblages (Backer et al., 2014; Boehlert and Gill, 2010; Kerckhof et al., 2011; Svane and Petersen, 2001)), offshore wind farms (OWFs) are known to produce potential impacts on a variety of ecosystem components of aquatic habitats (Degraer et al., 2013), such as alteration of the local biodiversity balance (Airoldi and Bulleri, 2011; De Mesel et al., 2015; Lloret et al., 2022) including changes to local primary production through facilitation of suspension feeders (Lloret et al., 2022; Mavraki et al., 2020; Slavik et al., 2019).

Some concern has been raised about the impacts of OWFs on the natural environment (Maar et al., 2009), notably on water quality. Suspended particulate matter (SPM) is an important indicator of water quality in turbid coastal areas (Liu et al., 2017). SPM includes all organic and inorganic suspended particles present in the water (Waters, 1995). SPM is crucial in describing water quality because it controls light penetration into the water column (hence affecting the growth conditions for marine phytoplankton), and also influences the adsorption/desorption of nutrients that facilitate eutrophication (He et al., 2017).

The impacts of OWFs on the water quality of the North Sea could be diverse (Clark et al., 2014; WWF-Norway, 2014) and are not yet fully understood. Some authors note that the impacts vary locally and per type of turbine (Degraer et al., 2013), while others suggest that impacts of OWFs on sediment plumes may take effects beyond local scales (Ivanov et al., 2021). Most reported impacts due to wind farms on the coastal shelf are changes to hydrodynamics and increased sediments in suspension around

* Corresponding author.
*E-mail addresses:* isabel.brandao@nioz.nl (I.L.S. Brandao), johan.van.der.molen@nioz.nl (J. van der Molen), daphne.van.der.wal@nioz.nl (D. van der Wal).

http://dx.doi.org/10.1016/j.scitotenv.2022.161114
Received 3 August 2022; Received in revised form 15 November 2022; Accepted 18 December 2022
Available online 29 December 2022

wind farm foundations (Ivanov et al., 2021). Recent studies have found that besides meteorological forcing and hydrodynamic conditions, seabed sediment composition is a key variable explaining SPM concentrations (Ivanov et al., 2021). In shallow areas (e.g., near the mouth of the Thames) with a muddy bed composition, increased sediment resuspension may result in large sediment plumes, as reported in Vanhellemont and Ruddick (2014). Sediment plumes around foundations, seen in shallow-water and high-current velocity systems, are not expected in deeper areas where hydrodynamics are less impacted by tidal forcing (Baeye and Fettweis, 2015; Degraer et al., 2013), as weaker bottom currents in such deeper waters reduce the potential scour and the time sediments remain suspended within the water column. In such conditions, sediment resuspension near foundations would not be measurable above existing natural/baseline conditions (Degraer et al., 2013). However, in addition to tidal currents, several other factors may influence the length of wakes, such as wave conditions, particle settling velocity, and artificial seafloor modifications (Vanhellemont and Ruddick, 2014).

Thus, SPM concentrations and their spatial, seasonal, and multi-annual fluctuations, combined with information on their hydrodynamic and climatic drivers and environmental conditions (such as water depth and seabed sediment composition), should be considered to understand the impacts of OWFs on the water quality of coastal shelf seas. Overall, the opportunity to determine SPM from satellite remote sensing data is attractive in these studies because satellite images provide a spatiotemporal synoptic view (Duan et al., 2019; Palmer et al., 2015), even though satellite data can only detect SPM in the near-surface layers of the water column. Moreover, light intensity and hence effects of SPM on primary production are highest in surface waters.

This study assessed the spatial and temporal patterns of SPM concentrations in OWF areas located in the Dutch part of the North Sea from satellite remote sensing. A Before-After Control-Impact (BACI) analysis was performed to investigate the impacts of the construction of the wind farms. BACI designs and analysis are effective at capturing changes over time (B: Before, A: After) and space (C: Control, I: Impact) because they test the hypothesis of the occurrence of a potential impact (Fisher et al., 2019). The environmental factors influencing SPM concentrations were analyzed using scatterplots and correlations. Scatterplots are suitable for revealing nonlinear relationships, which is expected when using dataset with complex structures such as environmental data sets (Sainani, 2016). Furthermore, scatterplots can reveal the presence of outliers, display trends and correlations between two variables, etc. (Keim et al., 2010; Mayorga and Gleicher, 2013).

Accordingly, the main goal of this study was to investigate whether SPM concentrations changed after wind farm construction, and to identify the environmental variables impacting SPM in the wind farm areas. The main hypothesis was that the placement of wind farms in offshore areas changes SPM concentrations in the surface waters, and that these concentrations are higher in the post-construction period.

## 2. Material and methods

### 2.1. Study area description

The study area is in the Dutch part of the North Sea (DPNS), which is part of a relatively shallow shelf sea (up to 50 m) that allows for strong interactions between physical and chemical processes in the water column (Noordzeeloket, 2012). The DPNS is also characterized by a river plume extending along the entire coast, containing suspended material (clay) responsible for the turbidity in this area (Rijnsburger et al., 2018). The North Sea is a site of ecological importance due to diverse marine life including commercial fish stocks, and the presence of large mudflats (such as those found in the Wadden Sea) supporting, e.g., a variety of migratory bird species (Álvarez et al., 2019; ICES, 2018; Kinne, 1995). The North Sea also has multiple uses such as shipping, oil and gas extraction, sand mining, fisheries, recreation, and wind farms (Capuzzo et al., 2018). These multiple uses provide economic growth to the densely populated countries surrounding the North Sea. The North Sea is an essential source of energy supply, and in times of climate change, this area has been increasingly targeted for future investments in offshore wind energy. In fact, wind farms in the North Sea represent 71 % of total European offshore wind energy production and the Netherlands recently contributed approximately 1120 MW to the rapidly expanding European wind energy generation capacity (De Castro et al., 2019).

While efforts are being made to understand the impacts of existing wind farms in offshore areas, many new wind farms are still being planned.

The wind farms built and in operation in the DPSN are Egmond aan Zee (EAZ-OWF), Princess Amalia (PA-OWF), Luchterduinen (L-OWF), Gemini (G-OWF) (Table 1) and Borssele. The highest offshore wind capacity is installed for the Borssele wind farm (1400 MW), followed by the Gemini wind farm (600 MW, see Table 1). The wind farms are located relatively close to the coast (21 km) except for the Gemini wind farm, which is located 85 km from the coast (Fig. 1). Although the Borssele wind farm, completed in 2019, is one of the largest Dutch OWFs, we are not considering it in this study, due to limited availability of cloud-free satellite images and model data of environmental variables covering the period of six years after its construction. Besides, sediment plumes originating from the Belwind wind farm, 0.5 km away in the Belgium Exclusive Economic Zone (EEZ), may influence the Borssele wind farm site, which would complicate the analysis.

The sediments in the DPNS are mainly composed of fine to medium sands with silt and, in some locations, mud additions (van der Spek et al., 2022). The sediment type varies per wind farm location, but there is a predominance of fine sand at Princess Amalia, Egmond aan Zee, and Luchterduinen, and coarse, medium and fine sand and mud at the Gemini wind farm (Ivanov et al., 2021).

### 2.2. Sample design

A sampling design was created to evaluate the impact of OWFs on suspended matter concentrations (Fig. 1), based on a Before-After Control-Impact (BACI) analysis and following the functionality of the 'epower' R package (Fisher et al., 2019). The criteria to determine control sites were that these should be located i) at similar depth and distance from the coast, and ii) relatively far from the impact sites (here, the operational wind farm) to ensure unmodified environmental conditions in space and time, so the controls can be considered independently monitored areas. In this investigation, the control sites were designed with the same shape and area as the nearby OWFs. Furthermore, impact and control sites were separated by a distance of approximately 15 km, which is the maximum length of reported SPM plumes (Przyborska et al., 2020). Depending on data availability, periods of approximately 6 years before and after construction of the wind farms were considered for each area.

**Table 1**
Operational wind farms in the Dutch part of the North Sea considered in this study.

| Wind farm | Coordinates | Capacity (MW) | Average water depth (m) | Construction year | Period (Before) | Period (After) |
|---|---|---|---|---|---|---|
| Luchterduinen | 52.4° N 4.2° E | 129 | 15.90 | 2015 | 2004–2013 | 2014–2020 |
| Princess Amalia | 52.6° N 4.2° E | 120 | 21.67 | 2008 | 2000–2006 | 2008–2014 |
| Egmond aan Zee | 52.6° N 4.4° E | 108 | 26.13 | 2007 | 2000–2006 | 2009–2016 |
| Gemini I | 54.0° N 6.0° E | 600 | 34.26 | 2015 | 2006–2014 | 2015–2019 |
| Gemini II | 54.0° N 5.9° E | | 33.36 | | | |

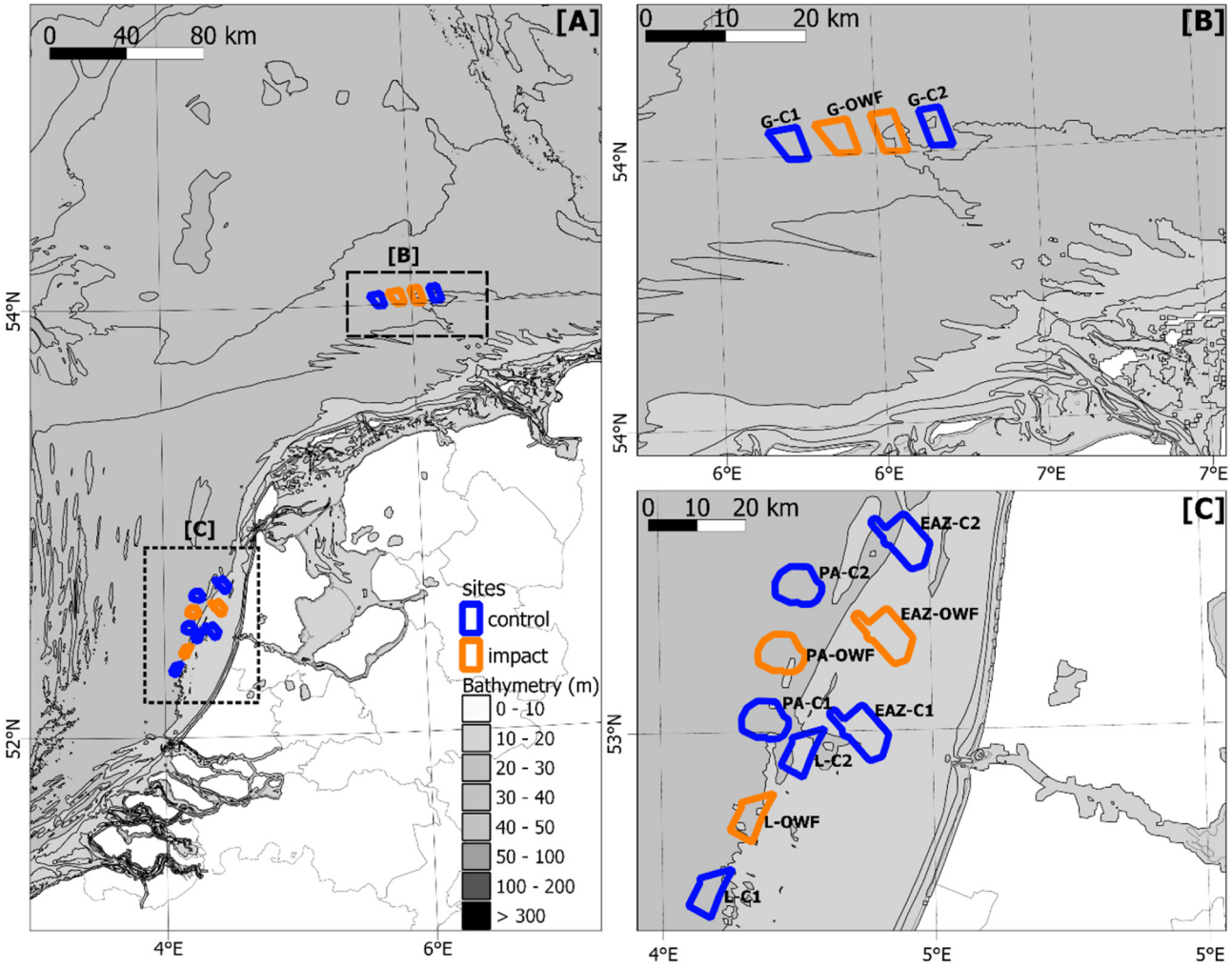


**Fig. 1.** Study sites including impact (in orange color) and controls (in blue color) and depth (in gray colors). Plot A shows the location of the wind farms in the North Sea. Plot B shows the Gemini wind farm (G-OWF). Plot C shows Princess Amalia (P-OWF) (on the left), Egmond aan Zee (EAZ-OWF) (on the right) and Luchterduinen (L-OWF) (lower center) wind farms. (For interpretation of the references to color in this figure legend, the reader is referred to the web version of this article.)

### 2.3. Variable selection and data sources

#### 2.3.1. Retrieval of SPM from satellite data

In this study, satellite data from the Thematic Mapper onboard of Landsat-5 (L5-TM), Landsat-7 (L7-ETM (Enhanced Thematic Mapper), and Landsat-8 (L8-OLI (Operational Land Imagery)) were acquired between 2000 and 2019 (Table 1). All three sensors have 30 m spatial resolution for the retrieval of SPM in the red channel (655 nm and 660 nm). Free orthorectified and terrain corrected Level 1 T imagery was obtained from the United States Geological Survey (USGS — https://earthexplorer.usgs.gov/). Collection 1 data from both Tiers 1 and 2 was used. Tier 1 includes the best quality scenes, including precision terrain correction and accurate georegistration (<12 m root mean square error). Tier 2 contains the other scenes that do not meet Tier 1 criteria because of cloud cover and lack of ground control points. Since offshore scenes often fall into Tier 2, both categories were used here.

Imagery atmospheric correction (AC) was processed with ACOLITE which is a free tool of the Royal Belgium Institute of Natural Science (RBINS) and it was developed in python 3 (Vanhellemont, 2019; Vanhellemont and Ruddick, 2018). In ACOLITE's settings we used an AC based on the "dark spectrum fitting" (DSF) technique developed by Vanhellemont and Ruddick, 2018 which estimates the best fitting aerosol model. The DSF was applied to individual tiles. Data were removed where water-leaving radiance $\rho_w < 0$ in any band, and where the water-leaving radiance in the SWIR (Short-Wave InfraRed) $\rho_{w,\,\lambda=1.6\mu m} > 0.01$ ($\lambda$ = band wavelength), as water-leaving radiance for this wavelength is expected to be negligible (Wang, 2007). Hence, contributions to the signal in the SWIR that could be attributed to atmospheric scattering, glint on the water surface, haze and clouds were flagged as non-data (Vanhellemont and Ruddick (2018).

The atmospheric correction of satellite data is very important when studying aquatic ecosystems because a large part of the detected signal by the sensor is also a contribution from the medium between the studied target and the atmosphere. Thus to properly retrieve any water quality variable, the atmospheric correction is a critical step in data processing of satellite images (Kutser et al., 2005; Perkins et al., 2012).

For the OWFs of the Dutch part of the North Sea, SPM concentration products were created by applying the approach of (Nechad et al., 2010b), calibrated for the North Sea (Table 2), to the tiles obtained from USGS Earth Explorer, and after atmospheric correction using ACOLITE, using

$$\mathrm{SPM} = \frac{A^{\rho} \cdot \rho_w}{1 - \frac{\rho_w}{C^{\rho}}}, \tag{1}$$

where $A^{\rho}$ and $C^{\rho}$ are band-specific calibration coefficients. These coefficients were calibrated for turbid waters by (Nechad et al., 2010a) (Table 2) and they are suitable for most ocean color sensors and sensors with the red channels as those found in the TM, ETM and OLI series (Vanhellemont, 2019).

**Table 2**
Sensor bands and their corresponding $A^{\rho}$ and $C^{\rho}$ coefficients from (Nechad et al., 2010b)) used to compute SPM from satellite imagery.

| Satellite/sensor | Bands (λ nm) | Spatial resolution (m) | Coefficients |
|---|---|---|---|
| Landsat-5 (TM); Landsat-7 (ETM) | 660 | 30 | $A^{\rho} = 327.84$; $C^{\rho} = 17.08$ |
| Landsat-8 (OLI) | 655 | 30 | $A^{\rho} = 289.29$; $C^{\rho} = 16.86$ |

Suspended matter concentrations were derived from satellite remote sensing data for the entire studied period. Composite maps of SPM, showing before and after conditions (Table 1), were created using the geometric mean as it is less sensitive to very high concentrations than other measures of central tendency (Eleveld et al., 2008).

Turbine footprints were masked out by a buffer of 5 x 5 bounding box size (where 1 pixel equals 30 × 30 m) to avoid reflectance signals from the monopiles and their rotor blades from affecting SPM concentrations. Then SPM $\log_{10}$ transformed mean values of each study site were calculated from each satellite scene (hereafter snapshots). Results of this procedure were used as input for the BACI analysis and for the boxplots. The analysis was also carried out using different bounding box sizes (5 x 5, 9 x 9, and 13 x 13 pixels) to explore the sensitivity of the results to the box size. These box sizes may show SPM changes due to local hydrodynamics (e.g., wind speed, currents).

#### 2.3.2. Deriving environmental variables from models

Hydrodynamic variables, including current velocity (m $s^{-1}$), temperature (°C) and salinity at the water surface layer, were derived from a model run of the same period as the satellite imagery with the north-west European continental shelf setup of the General Estuarine Transport Model (GETM) (Van der Molen et al., 2021), at a spatial resolution of approximately 5 × 5 km. GETM is an open-source model available from www.getm.eu and is described in detail in Burchard and Bolding (2002). Note that this model does not include the effects of wind farms. Wind speed (m $s^{-1}$) at 10 m height was selected as meteorological variable, and was obtained from the European Centre for Medium-Range Weather Forecasts (ECMWF) ERA-5 reanalysis, and interpolated to the same grid. The environmental variables were selected based on their well-documented influence on SPM concentrations in the North Sea (Baeye and Fettweis, 2015; Dobrynin et al., 2010; Eleveld et al., 2008; Forster, 2018; Pleskachevsky et al., 2005; Vanhellemont and Ruddick, 2014). All analyses of satellite remote sensing data and extraction of environmental variables from the GETM model were handled in the python program language using the following libraries: NumPy (Harris et al., 2020), datetime (Python, 2022), pandas (McKinney, 2010), and netCDF4 (Unidata, 2022). Environmental variables and satellite data were extracted for the before and after periods as shown in Table 1.

### 2.4. Statistical analysis

#### 2.4.1. Exploratory data analysis: SPM concentrations at each site

Satellite-derived SPM concentrations were investigated and compared among the sites using box plots and visual examination of spatiotemporal composites (i.e., composites of the median SPM concentration of the before and after periods). A Wilcoxon signed-rank test (McDonald, 2009) was used to determine whether the set of SPM data differed before and after the construction of the wind farms, applying a 5 % significance level.

#### 2.4.2. BACI analyses: testing for the effects of wind farms on SPM

A Before-After Control-Impact (BACI) (Underwood, 1992) design was applied to address whether the means of suspended matter concentrations differed between the periods before and after the construction of each set of wind farms. We used the epower package implemented in the R statistical language (Fisher et al., 2019), in RStudio (version 1.1.456). Epower consists of a power analysis using BACI contexts using a nested Laplace approximation-based approach for accurate numerical approximations to the posterior distributions of the parameters (Meekan et al., 2021; Myer and Johnston, 2019). Furthermore, epower provides an assessment of an impact by comparing two fitted Bayesian generalized linear mixed models (one with (BA ∗ CI) and one without (BA + CI) the BACI interaction term), with evaluation of the strength of the BACI interaction effect based on the posterior model probability of one model compared with the other (Meekan et al., 2021). Thus, a probability ratio of >0.5 provides more support for the BACI interaction model over a model with only the two non-interacting fixed effects (Fisher et al., 2019). All models of each set of OWF (Fig. 1) were fitted using default integrated nested Laplace approximation (INLA) priors and probability integration transform (PIT) plots used to assess each model. The BACI model selection was based on two criteria. First, a visual interpretation of the PIT plots was performed; the criterion is that these plots should resemble a uniform distribution given a 95 % confidence interval, if otherwise, the selected model is not appropriate for the data (Fisher et al., 2019). Second, the best model is chosen based on Deviance Information Criterion (DIC) and Watanabe-AIC (WAIC) Akaike Information Criterion. The WAIC and DIC are both information criteria, for which holds that the better models have the lowest WAIC and DIC (Evans, 2019; Spiegelhalter et al., 2002). BACI was performed for four offshore wind farm groups as shown in Fig. 1: Luchterduinen (L-OWF, L-C1, L-C2), Princess Amalia (PA-OWF, PA-C1, PA-C2), Egmond aan Zee (EAZ-OWF, EAZ-C1, EAZ-C2) and Gemini (G-OWF, G-C1,G-C2). The response variable was SPM (log10) concentration, and explanatory variables consisted of a time factor (BvA: before/after construction) and an area factor (CvI: control/impact site). Further, only days in which at least one control and impact site could be seen on the same satellite scene and under clear sky conditions were selected to avoid day-to-day variations in SPM concentration across sites.

Further model assessments consisted of determining the proportion of variance in SPM explained by the fixed effects of period (before-after) and treatment (control-impact), and their interaction effect (the BACI effect: $[control_{after} - control_{before}] - [impact_{after} - impact_{before}]$). We used the site-level (study site) as random to account for overdispersion. The significance of the BACI effect was performed using a parametric bootstrap method available in the RStudio pbkrtest package (Halekoh and Højsgaard, 2014).

#### 2.4.3. Exploratory analysis: environmental conditions at each site

Environmental variables were compared between individual sets of wind farms. A Wilcoxon signed-rank test was used to determine whether the satellite data sets used in this study were selected under similar environmental conditions in the data set before and after construction of the OWF, respectively. A 5 % significance level was applied.

#### 2.4.4. Correlation analysis: environmental variables correlated with SPM

Scatterplots and Spearman correlations were used to identify key variables correlated with suspended matter at the different sites. In total, five environmental variables were selected: salinity, temperature, wind speed, and current velocity. Data were arranged by season: summer (21/06–21/09), autumn (22/09–21/12), winter (22/12–21/03), and spring (22/03–22/06). The visual inspection was performed in python using seaborn (Waskom, 2021) and matplotlib (Hunter, 2007) libraries. A 5 % significance level was applied for the Spearman correlations. Significant correlations were considered poor when $r \leq 0.3$ (Akoglu, 2018).

## 3. Results

### 3.1. SPM concentrations for each site

The Luchterduinen (L-OWF, L-C1, L-C2), Princess Amalia (PA-OWF, PA-C1, PA-C2), Egmond aan Zee (EAZ-OWF, EAZ-C1, EAZ-C2), Gemini (G-OWF, G-C1, G-C2) had mean SPM concentrations of 0.82 ± 0.22 g $m^{-3}$, 0.83 ± 0.20 g $m^{-3}$, 0.82 ± 0.25 g $m^{-3}$ and 0.68 ± 0.26 g $m^{-3}$ respectively considering the entire studied period (2000–2019) (Fig. S.1). The

greatest SPM variability was observed for the Gemini group with a coefficient of variation equal to 35.71 %. Note that no snapshots were available in autumn for the Gemini wind farm set.

The results of the Wilcoxon test showed that SPM for all windfarms and control areas had significantly different median values in the period before versus after construction of the OWFs ($median_{before}$ = 0.87 g $m^{-3}$;

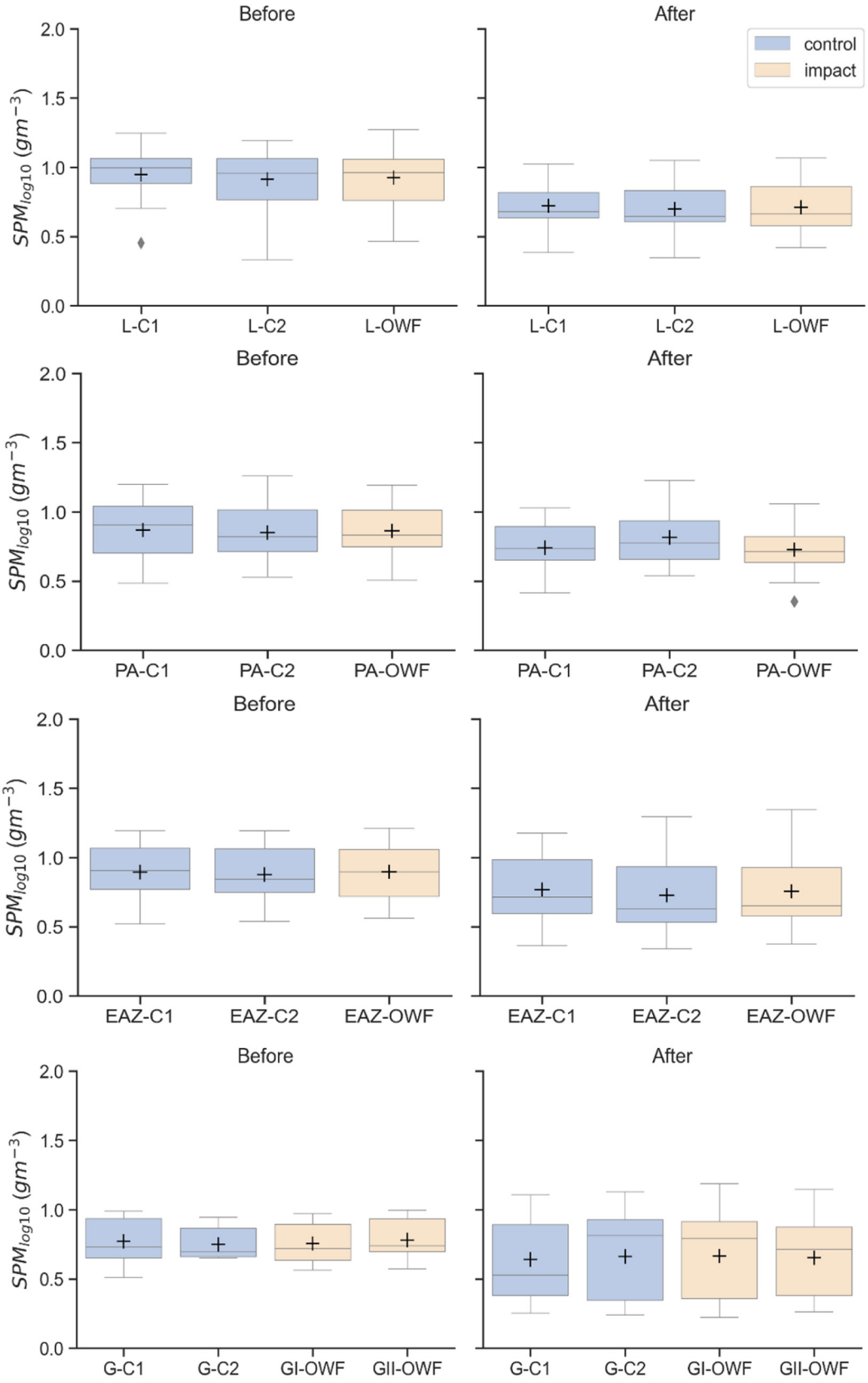


**Fig. 2.** Boxplots showing SPM concentration across offshore wind farm and their respective control areas, respectively before and after construction of the wind farms. The cross signs (+) are the median values. Further information about these results is also given in the Supplementary Tables S.1 and S.2.

$median_{after} = 0.72\ g\ m^{-3}$), with $p$-values < 0.0001. When individual sets of wind farms (OWF + control sites) were graphically compared, we could observe that SPM concentrations did not vary substantially among them, though slightly maximum values of SPM were observed in the after period, for instance, at the EAZ-C2 and EAZ-OWF. The range of the whisker length for the boxplots in Fig. 2 represents the maximum values of SPM.

The composites of SPM across impact and control sites show visual changes for the Luchterduinen, Princess Amalia, and Egmond aan Zee wind farms with slightly lower concentrations (bluer colors) after the construction of these wind farms, except for the EAZ-C2. SPM concentrations across Gemini wind farm and controls (in the lower panel) show minor spatio-temporal variations (Fig. 3).

The analysis of turbine footprint considering a buffer of different bounding box sizes (5 × 5, 9 × 9, 13 × 13) to avoid strong reflectance signals from their monopiles revealed no significant differences ($\chi^2$ = 0.52, $p$-value = 0.78) in the median values of SPM.

### 3.2. BACI analyses: the effects of wind farms on SPM

The BACI analysis statistically tests the difference in SPM level before and after in each set of wind farm (OWF + control sites). Wilcoxon test results showed that SPM concentrations were significantly different when comparing before (median value of the SPM = 0.87 g $m^{-3}$) and after periods (median = 0.69 g $m^3$) with $p$-value < 0.0001, while

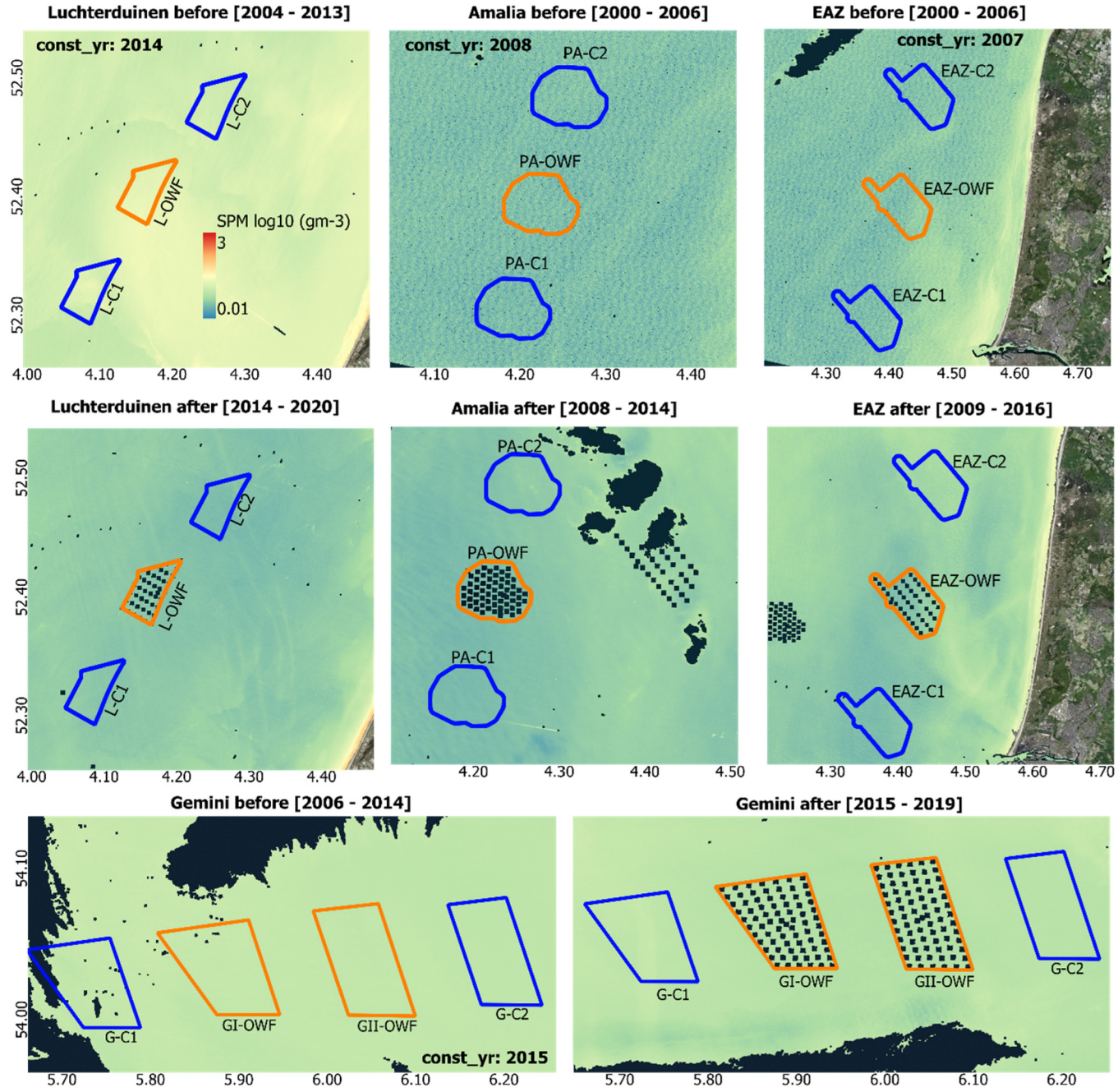


**Fig. 3.** Temporal composites of suspended particulate matter before and after the construction of the Dutch offshore wind farms (const_yr = construction year). Control sites are highlighted in blue color and impact sites in orange color. Squared black patches inside of the wind farms are masked out monopile footprint (5 × 5 window size) and black patches without shape are clouds and cloud shadows removed by the atmospheric correction. (For interpretation of the references to color in this figure legend, the reader is referred to the web version of this article.)

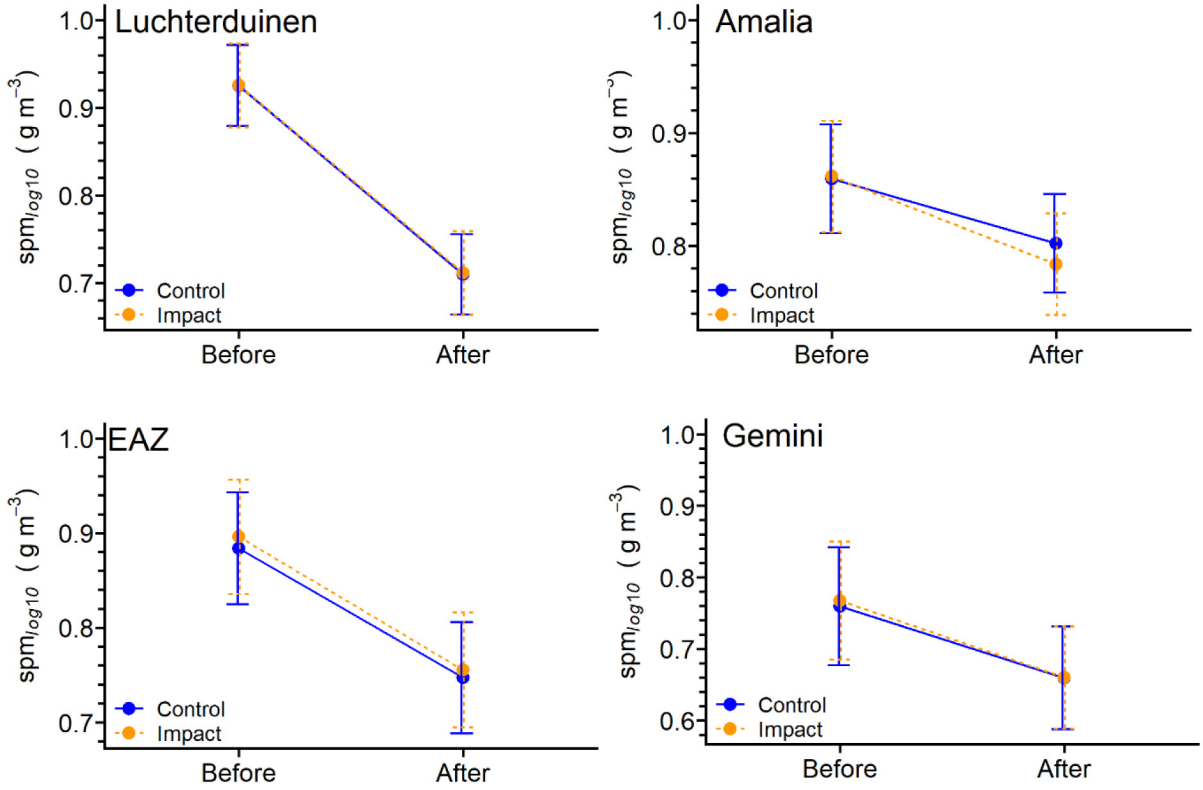


**Fig. 4.** Modelling results of the BACI analysis showing SPM mean estimates (±SD) for each set of offshore wind farm located in the Dutch part of the North Sea.

no significant differences were observed when comparing control (median = 0.79 g m$^{-3}$) and impact sites (median = 0.76 g m$^{-3}$) with $p$-value = 0.46.

The stronger decrease in SPM for before period as compared to after period, for impact and control sites was not large enough for the BACI analysis (Fig. 4) to detect it as a significant change considering a CI of 95 % (Appendices Tables A.1 to A.4). At Luchterduinen, the estimated mean SPM values in the impact site dropped from 0.968 to 0.756, while in the control sites, it dropped from 0.970 to 0.753; the BACI effect estimated was −0.005 ± 0.076. At Princess Amalia, the estimated mean SPM values in the impact site dropped from 0.891 to 0.833, while in the control sites, it dropped from 0.894 to 0.843; the BACI effect estimated was 0.007 ± 0.094. At Egmond aan Zee, the estimated mean SPM values in the impact site dropped from 0.907 to 0.871, while in the control sites, it dropped from 0.893 to 0.849; the BACI effect was −0.008 ± 0.079. At Gemini, the estimated mean SPM values in the impact site dropped from 0.808 to 0.763, while in the control sites, it dropped from 0.800 to 0.759; the BACI effect was 0.004 ± 0.086. The BACI effect [control$_{after}$ − control$_{before}$] − [impact$_{after}$ − impact$_{before}$] estimated for all study sites did not detect significant changes in SPM concentrations.

### 3.3. Environmental variables for each site

The sites differed in environmental conditions (Table 3). Highest current velocities were found at the Amalia wind farm PA-OWF, while lowest values were identified at Gemini-OWF and control sites G-C1 and G-C2. Highest wind speeds were observed for G-C1, with mean values of 5.92 m s$^{-1}$, and lowest values for Luchterduinen control site L-C2, with mean values of 4.41 m s$^{-1}$. When pairwise compared, significant differences in the median values of wind speed were observed for impact sites PA-OWF and L-OWF ($p$-value = 0.004); G-OWF and L-OWF ($p$-value < 0.001) and EAZ-OWF and G-OWF ($p$-value = 0.04). Note that the differences in environmental conditions between sites do not reflect the presence of wind farms, as this is not taken into account in the model.

Temperature (median$_{before}$ = 16.74 °C; median$_{after}$ = 9.92 °C) and salinity (median$_{before}$ = 30.12; median$_{after}$ = 31.11) were significantly

**Table 3**
Mean, standard deviation (±SD), and coefficient of variation (CV%) of the environmental variables influencing SPM concentration averaged over snapshots coinciding with the satellite data for the entire studied period (2000–2019) of OWFs and control sites. More information can be found on the Supplementary Tables S.1 and S.2.

| Site | Current velocity (m s$^{-1}$) | CV | Salinity | CV | Temperature (°C) | CV | Wind speed (m s$^{-1}$) | CV |
|---|---|---|---|---|---|---|---|---|
| L-OWF | 0.46 ± 0.20 | 43.48 | 29.97 ± 1.24 | 4.14 | 12.46 ± 5.63 | 45.18 | 4.36 ± 1.84 | 42.20 |
| L-C1 | 0.51 ± 0.22 | 43.14 | 29.28 ± 1.76 | 6.01 | 12.67 ± 5.59 | 44.86 | 4.36 ± 1.77 | 40.60 |
| L-C2 | 0.47 ± 0.19 | 40.43 | 30.26 ± 1.09 | 3.60 | 12.46 ± 5.64 | 45.26 | 4.41 ± 1.86 | 42.18 |
| PA-OWF | 0.51 ± 0.20 | 39.22 | 30.60 ± 1.26 | 4.12 | 13.06 ± 5.43 | 41.58 | 5.37 ± 2.25 | 41.90 |
| PA-C1 | 0.51 ± 0.21 | 41.18 | 30.28 ± 1.39 | 4.59 | 12.94 ± 5.41 | 41.81 | 5.30 ± 2.23 | 42.03 |
| PA-C2 | 0.52 ± 0.20 | 38.46 | 31.03 ± 1.29 | 4.16 | 12.89 ± 5.39 | 41.82 | 5.39 ± 2.32 | 43.04 |
| EAZ-OWF | 0.44 ± 0.18 | 40.91 | 29.30 ± 1.01 | 3.45 | 13.32 ± 5.83 | 43.77 | 4.71 ± 1.85 | 39.28 |
| EAZ-C1 | 0.45 ± 0.18 | 40.00 | 29.21 ± 1.05 | 3.59 | 13.32 ± 5.81 | 43.62 | 4.59 ± 1.82 | 36.65 |
| EAZ-C2 | 0.45 ± 0.19 | 42.22 | 30.31 ± 1.08 | 3.56 | 13.27 ± 5.78 | 43.56 | 4.87 ± 1.90 | 39.01 |
| G-OWF | 0.31 ± 0.16 | 51.61 | 33.68 ± 0.62 | 1.84 | 11.94 ± 5.47 | 45.81 | 5.81 ± 2.71 | 46.64 |
| G-C1 | 0.32 ± 0.15 | 48.39 | 33.94 ± 0.72 | 2.12 | 12.14 ± 5.40 | 44.48 | 5.92 ± 2.65 | 44.76 |
| G-C2 | 0.32 ± 0.17 | 53.13 | 33.22 ± 0.59 | 1.78 | 11.76 ± 5.52 | 46.94 | 5.70 ± 2.77 | 48.60 |

different in the data set before versus after construction, with $p$-values < 0.0001. As the wind farms are not considered in the modelled environmental variables (such as temperature and salinity), this suggests that the data before and after are acquired under different environmental forcing.

### 3.4. Environmental variables correlated with SPM

Visual inspection identified significant, but poor correlations between satellite-derived SPM and co-occurring environmental variables — current velocity, wind speed, temperature, and salinity (Fig. 5). Our results showed a strong seasonal effect of the environmental variables on SPM concentrations at all sites with coincident satellite snapshots (Supplementary Fig. S.1). In general, high SPM values were observed in autumn (median = 1.01 g $m^{-3}$) and winter (median = 0.82 g $m^{-3}$), in accordance with higher wind speed (autumn = 6.17 m $s^{-1}$; winter = 6.13 m $s^{-1}$) compared to other seasons (Fig. 5). The highest positive and significant correlations of SPM and wind speed were observed in spring at Gemini ($r_{Spearman} = 0.84$, $p < 0.0001$). In summer, SPM values were poorly correlated to the environmental variables at the site scale. In autumn, only the Princess Amalia sites showed correlation between SPM and more than one environmental variable: at these sites, strong negative correlations were found between SPM and current velocity ($r_{Spearman} = -0.73$, $p = 0.001$) and temperature ($r_{Spearman} = -0.58$, $p = 0.011$) and positive correlations with salinity ($r_{Spearman} = 0.70$, $p = 0.001$). In winter months, moderate negative correlations were observed between SPM and temperature at the Gemini ($r_{Spearman} = -0.74$, $p = 0.001$) and Princess Amalia ($r_{Spearman} = -0.67$, $p = 0.001$) sites; and between SPM and current velocity ($r_{Spearman} = -0.54$, $p = 0.02$) and wind speed ($r_{Spearman} = -0.56$, $p = 0.02$) at the Egmond aan Zee sites (Fig. 5). Further information on the seasonality for before and after periods is given in the Supplementary material (S.5 and S.6).

## 4. Discussions

In this study, we investigated the impacts of OWFs on the water quality of coastal areas, and the variable suspended particulate matter was used to assess the impact of these wind farms. Therefore, a BACI design was proposed to evaluate changes between impacts and control sites in the pre- and post-wind farm construction periods and a visual inspection of scatterplots to investigate which combination of environmental variables influences SPM concentrations within OWF areas.

The results of the BACI analysis revealed that a change occurred in SPM concentrations considering the Before and After periods, and these changes are visible on the composite satellite data. In that, statistical comparisons revealed that our sets of satellite imagery have not been acquired under similar environmental conditions, as temperature and salinity were significantly different in the before and after periods, potentially explaining such differences in SPM.

The geometric mean was used to create composite maps of SPM because it is less sensitive to extremely high concentrations than other measures of central tendency; however, we noticed that this measure may have influenced the findings in Fig. 3. Snapshots with extremely high SPM values may have had an impact on the composite for the EAZ wind farm set after-period. The use of geometric mean in satellite data reduction (e.g., composites) has been reported to introduce bias when a small data set is used or it tends to overestimate pixel values when the data is contaminated with speckles (Park et al., 2012).

Our BACI analyses did not reveal any significant differences in SPM concentrations in response to wind farm construction. We therefore could not confirm our main hypothesis that turbidity and SPM increased (e.g., due to a change in hydrodynamics) around the wind farms. The BACI analysis assumes that the selected model represents an adequate fit by looking at the Probability Integral Transform (PIT) plots. These plots ought to adhere to a typical uniform distribution (Fisher et al., 2019). The selection of the PITs may have added uncertainties to the final outputs. The lower SPM concentrations after construction of the OWF Princess Amalia as compared to its controls were also not significant. We considered the effects of wind farms on SPM within a ca 6-year period. It is possible that effects on SPM manifest themselves following construction (Degraer et al., 2013). For example, a decrease in SPM can be caused by the establishment of an assemblage of filter feeders which have the capability to remove large amounts of SPM from the water column (Krone et al., 2013). Ivanov et al. (2021) suggest in a modelling study that SPM content is higher along the coast than in the offshore zone – where the Dutch wind farms are located. Zijl et al. (2021, in fig. 6.3) showed in a study encompassing modelled scenarios with the presence of wind farms in the DPNS for 2020 and 2050, that in the scenario for 2020 (where hydrodynamic changes and mussel growth were considered), sea surface SPM concentrations decreased in most parts of the Rhine ROFI area, where our study sites are located.

The visual inspection of scatterplots showed that season greatly contributes to SPM patterns in the studied area. SPM concentrations are known to differ by season in the North Sea, with increased surface concentrations in autumn and winter and lower values in spring and summer (Eleveld et al., 2008; Pietrzak et al., 2011), and with winter months showing the highest SPM concentrations associated with enhanced resuspension by wind waves (e.g.,(Van der Molen et al., 2017)). In contrast, our study showed the highest SPM values in autumn. As a result, the correlation between temperature and SPM concentration is coincidental as both vary with season but by different environmental drivers. There may be an occasional secondary contribution of temperature on SPM concentrations in the Rhine ROFI area in summer when salinity-stratified surface waters receive additional warming, creating a pycnocline that traps SPM in the bottom layer (Pietrzak et al., 2011).

Overall, the scatterplots show a complex relationship between SPM and environmental variables. For instance, it seems that higher median values of wind speeds are responsible for higher SPM concentrations in spring and winter months, while lower wind speeds correlate with lower SPM concentrations in summer months. High wind speeds are observed primarily in storm conditions, which is most likely observed in the autumn for this region. We observed low SPM values in summer, associated with less storm activity and low wind speeds. While peaks of SPM have usually been reported in winter (Pietrzak et al., 2011), in this study, we found similar concentrations in both autumn and winter seasons, which could be related to 1) changes in environmental forcing or 2) due to low satellite data availability for the winter season. We assume that using more frequent satellite observations such as those of Sentinel-2 or the use of commercial satellite (e.g., Planet constellation) would greatly reduce uncertainties caused by the lack of data availability. Unfortunately, the Sentinel-2 satellite was launched after the installation of the wind farms used in this study, making it difficult to use its observations.

Wind speed (which is expected to highly affect SPM concentration in the ROFI region in winter months due to increased resuspension (Pietrzak et al., 2011)), showed a moderate negative correlation with SPM at the Egmond aan Zee OWF ($r_{Spearman} = -0.56$, $p = 0.02$). However, in spring months, positive and significant correlations were observed at the Gemini OWF ($r_{Spearman} = 0.84$, $p < 0.0001$). The Rhine ROFI is well-mixed after stormy conditions and usually shows increased SPM concentrations right after such events, as observed in a 20 years study on SPM concentrations (Suijlen and Duin, 2002). However, it is worth mentioning that the SPM concentrations derived from satellite sensors, in this study, mostly used scenes acquired during calm weather conditions (wind speed = 4.91 ± 2.14 m $s^{-1}$). Furthermore, our results suggest that SPM concentrations are highly dynamic and dependent on season, meteorological and hydrodynamic forcing in this study area, thus demanding the use of high temporal and spatial resolution sensors to capture the complexity of the plumes, including the settling lags of SPM.

Compared to what has been observed in other locations, such as the English coast (Vanhellemont and Ruddick, 2014), in our 20-year satellite data of the Dutch OWFs, we could observe only a few scenes where SPM plumes related to wind turbines were registered by the sensors used in this study at very low overall SPM concentrations (Figs. S3 and S4). These differences might be explained by differences in the bed composition and effects of stratification between these two locations. The Dutch OWFs are in the

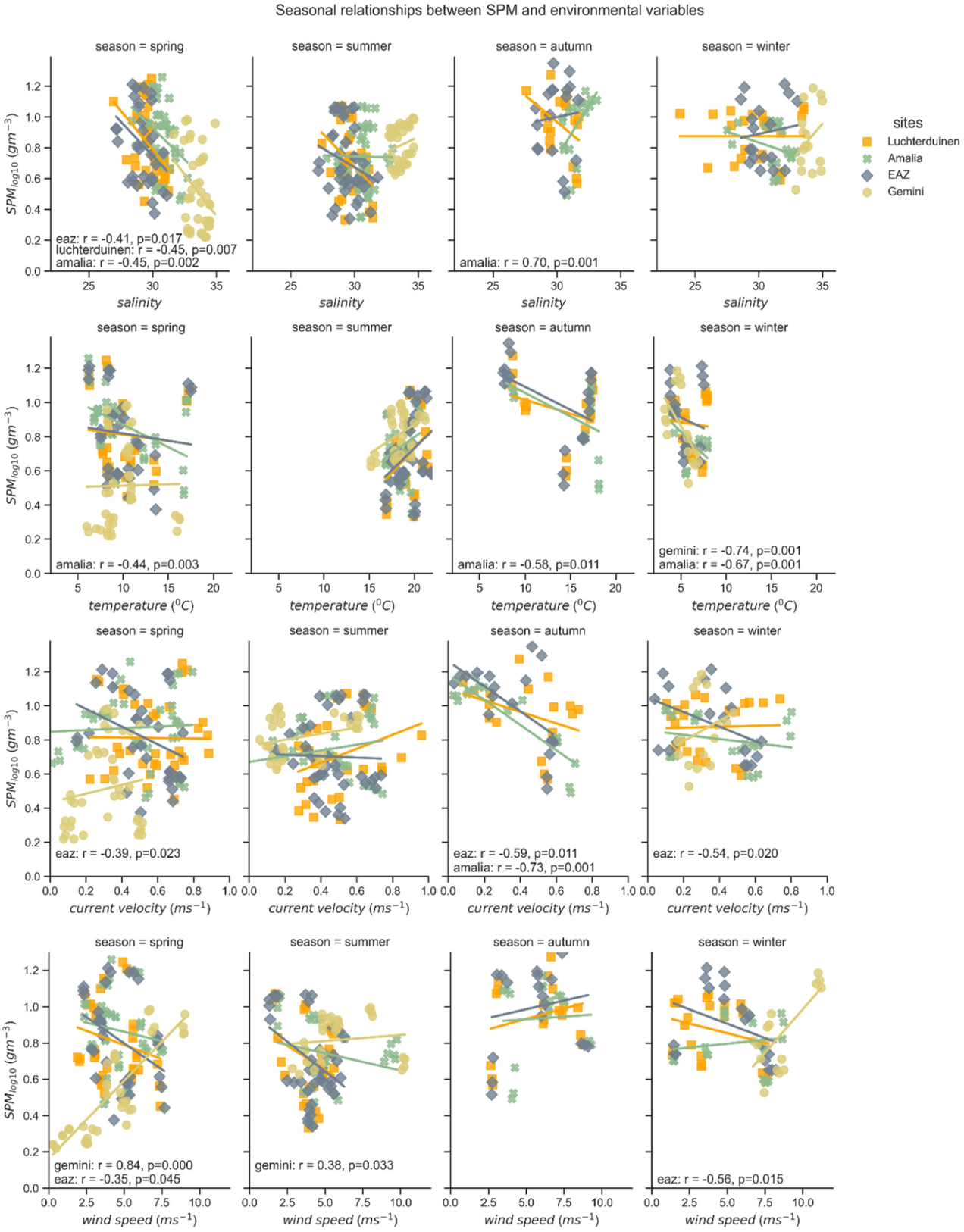


**Fig. 5.** Seasonal relationships between suspended particulate matter and co-occurring environmental variables at each site. No snapshots were available in autumn for the Gemini-OWF and only significant correlations are shown ($p \leq 0.05$).

ROFI region, where fine sand is predominant and intermittent seasonal stratification is observed; thus, it may be less likely that SPM plumes will be frequently observed around these wind farms. It is possible that plumes are also present in stratified conditions but confined to the bottom mixed layer (and hence invisible by remote sensing). In contrast, the wind farms located on the English coast have more influence on finer grained sediments (e.g., mud and silt) and considerable shear stress that may be causing resuspension of the deposited material (Stanev et al., 2009). Further

research, on a wide range of OWF's under different conditions, may employ our methods to test whether wind farms placed in sandy beds and under weak stratification are likely to cause less resuspension of the deposited material, hence minor visible SPM plumes. Such an extension of the current research could help with the planning of wind farms in offshore areas to avoid environmental impacts (e.g., SPM plumes).

## 5. Conclusions

A Before-After-Control-Impact design was used to investigate the effects of wind farms on the water quality of offshore areas, and an inspection of scatterplots and correlations to establish relationships between SPM and hydrodynamic and meteorological variables.

The spatio-temporal analysis using satellite imagery composites of before and after periods showed that SPM concentrations vary across wind farm sets in both before and after periods of sampling collection. SPM is biased by sampling under clear-sky and low wind conditions and SPM was acquired under different environmental conditions when comparing the data set before and after wind farms construction.

The scatterplots revealed that the main environmental variables correlating with SPM in the Dutch part of the North Sea are temperature and wind speed, and that these correlations differ for each season. It should be noted that the modelled meteorological and environmental variables used did not include the presence of the wind farms and that no satellite snapshots were available for the Gemini OWF in autumn.

The BACI analysis revealed changes in SPM concentrations when comparing a period of approximately 6 years before and after wind farm construction, while no significant changes were observed when comparing control and impact treatment. Furthermore, the BACI analysis thus did not reveal any significant effect on SPM in response to the construction of the wind farms.

The BACI analysis thus proved helpful for determining changes in water quality (e.g., through SPM) due to OWFs and the visual inspection of scatterplots for determining what set of environmental variables influenced SPM concentrations. The combination of these two approaches provided crucial information that can support the water quality monitoring in impacted areas. In addition, satellite imagery was crucial in providing SPM data at various spatio-temporal scales and that using different bounding box sizes (5 × 5, 9 × 9 and 13 × 13 pixels of 30 × 30 m) was not an important factor to explain SPM variation around wind farms.

## CRediT authorship contribution statement

ILSB designed the study, performed the research and wrote the manuscript. DVDW designed the study, supervised and coordinated the study and contributed to the writing and editing of the manuscript. JVDM led the project this study was part of and contributed to the editing of the manuscript. All authors approved the submitted version.

## Funding

This work was funded by the Netherlands Organization for Scientific Research (NWO) as part of the 'Nationale Wetenschapsagenda L2 - NWA 2018 - Ecologie & Noordzee' programme under grant number NWA.1236.18.001.

## Data availability

Data will be made available on request.

## Declaration of competing interest

The authors declare no conflict of interest. The sponsors had no role in the design of the study; in the collection, analyses, or interpretation of data; in the writing of the manuscript; or in the decision to publish the results.

## Acknowledgments

The authors would like to thank the Netherlands Organization for Scientific Research (NWO) and the Royal Netherlands Institute for Sea Research (NIOZ) for their support with the funding; Quinten Vanhellemont (RBINS) with his support and assistance with conducting atmospheric correction using ACOLITE; Bas Retsios (Faculty of Geo-Information Science and Earth Observation, University of Twente) for his guidance in automating data processing. We thank the anonymous reviewers for their careful reading of our manuscript and their many insightful comments and suggestions.

## Appendix A. Supplementary data

Supplementary data to this article can be found online at https://doi.org/10.1016/j.scitotenv.2022.161114.

## References

Airoldi, L., Bulleri, F., 2011. Anthropogenic disturbance can determine the magnitude of opportunistic species responses on marine urban infrastructures. PLoS One 6, e22985.
Akoglu, H., 2018. User's guide to correlation coefficients. Turkish journal of emergency medicine 18, 91–93.
Álvarez, H., Perry, A.L., Blanco, J., Garcia, S., Aguilar, R., 2019. Protecting the North Sea: New Research for Biodiversity Recovery, p. 20 MarXiv, Madrid.
Backer, A.D., Van Hoey, G., Coates, D., Vanaverbeke, J., Hostens, K., 2014. Similar diversity-disturbance responses to different physical impacts: three cases of small-scale biodiversity increase in the Belgian part of the North Sea. Mar. Pollut. Bull. 84, 251–262.
Baeye, M., Fettweis, M., 2015. In situ observations of suspended particulate matter plumes at an offshore wind farm, southern North Sea. Geo-Mar. Lett. 35, 247–255.
Boehlert, G.W., Gill, A.B., 2010. Environmental and ecological effects of ocean renewable energy development: a current synthesis. Oceanography 23, 68–81.
Burchard, H., Bolding, K., 2002. GETM–a general estuarine transport model. Scientific Documentation. EUR, p. 20253 C3S ECfM-RWF. 2017.
Capuzzo, E., Lynam, C.P., Barry, J., Stephens, D., Forster, R.M., Greenwood, N., et al., 2018. A decline in primary production in the North Sea over 25 years, associated with reductions in zooplankton abundance and fish stock recruitment. Glob. Chang. Biol. 24, e352–e364.
Clark, S., Schroeder, F., Baschek, B., 2014. The Influence of Large Offshore Wind Farms on the North Sea and Baltic Sea: A Comprehensive Literature Review. Helmholtz-Zentrum Geesthacht, Zentrum für Material-und Küstenforschung.
De Castro, M., Salvador, S., Gómez-Gesteira, M., Costoya, X., Carvalho, D., Sanz-Larruga, F.J., et al., 2019. Europe, China and the United States: three different approaches to the development of offshore wind energy. Renew. Sust. Energ. Rev. 109, 55–70.
De Mesel, I., Kerckhof, F., Norro, A., Rumes, B., Degraer, S., 2015. Succession and seasonal dynamics of the epifauna community on offshore wind farm foundations and their role as stepping stones for non-indigenous species. Hydrobiologia 756, 37–50.
Degraer, S., Brabant, R., Rumes, B., Vigin, L., 2013. Environmental Impacts of Offshore Wind Farms in the Belgian Part of the North Sea. Learning From the Past to Optimise Future Monitoring. Available at:Royal Belgian Institute of Natural Sciences. http://odnature.naturalsciences.be/winmonbe2013/report.
Dobrynin, M., Gayer, G., Pleskachevsky, A., Günther, H., 2010. Effect of waves and currents on the dynamics and seasonal variations of suspended particulate matter in the North Sea. J. Mar. Syst. 82, 1–20.
Duan, H., Cao, Z., Shen, M., Liu, D., Xiao, Q., 2019. Detection of illicit sand mining and the associated environmental effects in China's fourth largest freshwater lake using daytime and nighttime satellite images. Sci. Total Environ. 647, 606–618.
Eleveld, M.A., Pasterkamp, R., van der Woerd, H.J., Pietrzak, J.D., 2008. Remotely sensed seasonality in the spatial distribution of sea-surface suspended particulate matter in the southern North Sea. Estuar. Coast. Shelf Sci. 80, 103–113.
Evans, N.J., 2019. Assessing the practical differences between model selection methods in inferences about choice response time tasks. Psychon. Bull. Rev. 26, 1070–1098.
Fisher, R., Shiell, G.R., Sadler, R.J., Inostroza, K., Shedrawi, G., Holmes, T.H., et al., 2019. epower: an r package for power analysis of before-after-control-impact (BACI) designs. Methods Ecol. Evol. 10, 1843–1853.
Forster, R., 2018. The Effect of Monopile-Induced Turbulence on Local Suspended Sediment Patterns Around UK Wind Farms: Field Survey Report. An IECS Report to The Crown Estate.
GWE C, 2010. Global wind power boom continues despite economic woes. Global Wind Energy Council (GWEC), Brussels, Belgium 68 pp http://www.gwec.net/fileadmin/documents/PressReleases/PR_2010/Annex%20stats%20PR%202009.pdf.
Halekoh, U., Højsgaard, S., 2014. A Kenward-Roger approximation and parametric bootstrap methods for tests in linear mixed models–the R package pbkrtest. J. Stat. Softw. 59, 1–32.
Harris, C.R., Millman, K.J., van der Walt, S.J., Gommers, R., Virtanen, P., Cournapeau, D., et al., 2020. Smith 474 nj. Kern R, Picus M, Hoyer S, van Kerkwijk MH, Brett M, Haldane A, del R'ıo JF, Wiebe M, Peterson P, G'erard-475 Marchant P, et al. Array programming with NumPy. Nature 585, 357–362.
He, Q., Qiu, Y., Liu, H., Sun, X., Kang, L., Cao, L., et al., 2017. New insights into the impacts of suspended particulate matter on phytoplankton density in a tributary of the Three Gorges Reservoir,China. Sci. Rep. 7, 13518.
Hunter, J.D., 2007. Matplotlib: a 2D graphics environment. Comput. Sci. Eng. 9, 90–95.
ICES, 2018. Greater North Sea Ecorregion - Ecosystems Overview. vol 6.

IPCC, 2022. Climate change 2022: mitigation of climate change. In: Shukla JS, P.R., Slade, R., Khourdajie, A. Al, van Diemen, R., McCollum, D., Pathak, M., Some, S., Vyas, P., Fradera, R., Belkacemi, M., Hasija, A., Lisboa, G., Luz, S., Malley, J. (Eds.), Contribution of Working Group III to the Sixth Assessment Report of the Intergovernmental Panel on Climate Change. Cambridge University Press, Cambridge, UK and New York, USA.
Ivanov, E., Capet, A., De Borger, E., Degraer, S., Delhez, E.J.M., Soetaert, K., et al., 2021. Offshore wind farm footprint on organic and mineral particle flux to the bottom. Front. Mar. Sci. 8, 614.
Keim, D.A., Hao, M.C., Dayal, U., Janetzko, H., Bak, P., 2010. Generalized scatter plots. Inf. Vis. 9, 301–311.
Kerckhof, F., Degraer, S., Norro, A., Rumes, B., 2011. Offshore Intertidal Hard Substrata: A New Habitat Promoting Non-indigenous Species in the Southern North Sea: An Exploratory Study. Offshore Wind Farms in the Belgian Part of the North Sea: Selected Findings From the Baseline and Targeted Monitoring. Royal Belgian Institute of Natural Sciences, Management Unit of the North Sea Mathematical Models, Marine Ecosystem Management Unit, Brussels, pp. 27–37.
Kinne, O., 1995. Ecology of the North Sea: problems, successes, failures, future needs. Helgoländer Meeresun. 49, 303–312.
Krone, R., Gutow, L., Joschko, T.J., Schröder, A., 2013. Epifauna dynamics at an offshore foundation–implications of future wind power farming in the North Sea. Mar. Environ. Res. 85, 1–12.
Kutser, T., Pierson, D.C., Kallio, K.Y., Reinart, A., Sobek, S., 2005. Mapping lake CDOM by satellite remote sensing. Remote Sens. Environ. 94, 535–540.
Liu, H., Li, Q., Shi, T., Hu, S., Wu, G., Zhou, Q., 2017. Application of Sentinel 2 MSI images to retrieve suspended particulate matter concentrations in Poyang Lake. Remote Sens. 9.
Lloret, J., Turiel, A., Solé, J., Berdalet, E., Sabatés, A., Olivares, A., et al., 2022. Unravelling the ecological impacts of large-scale offshore wind farms in the Mediterranean Sea. Sci. Total Environ. 824, 153803.
Maar, M., Bolding, K., Petersen, J.K., Hansen, J.L.S., Timmermann, K., 2009. Local effects of blue mussels around turbine foundations in an ecosystem model of Nysted off-shore wind farm,Denmark. J. Sea Res. 62, 159–174.
Mavraki, N., Degraer, S., Vanaverbeke, J., Braeckman, U., 2020. Organic matter assimilation by hard substrate fauna in an offshore wind farm area: a pulse-chase study. ICES J. Mar. Sci. 77, 2681–2693.
Mayorga, A., Gleicher, M., 2013. Splatterplots: overcoming overdraw in scatter plots. IEEE Trans. Vis. Comput. Graph. 19, 1526–1538.
McDonald, J.H., 2009. Handbook of Biological Statistics. vol 2. Sparky House Publishing, Baltimore, MD.
McKinney, W., 2010. Data Structures for Statistical Computing in Python. 445, pp. 51–56 Austin, TX.
Meekan, M.G., Speed, C.W., McCauley, R.D., Fisher, R., Birt, M.J., Currey-Randall, L.M., et al., 2021. A large-scale experiment finds no evidence that a seismic survey impacts a demersal fish fauna. Proc. Natl. Acad. Sci. 118.
Myer, M.H., Johnston, J.M., 2019. Spatiotemporal bayesian modeling of West Nile virus: identifying risk of infection in mosquitoes with local-scale predictors. Sci. Total Environ. 650, 2818–2829.
Nechad, B., Ruddick, K., Park, Y., 2010a. Calibration and validation of a generic multisensor algorithm for mapping of total suspended matter in turbid waters. Remote Sens. Environ. 114, 854–866.
Nechad, B., Ruddick, K.G., Park, Y., 2010b. Calibration and validation of a generic multisensor algorithm for mapping of total suspended matter in turbid waters. Remote Sens. Environ. 114, 854–866.
Noordzeeloket, 2012. Marine Strategy for the Netherlands Part of the North Sea 2012-2020, Part 1. 2022, Netherlands.
Palmer, S.C.J., Odermatt, D., Hunter, P.D., Brockmann, C., Présing, M., Balzter, H., et al., 2015. Satellite remote sensing of phytoplankton phenology in Lake Balaton using 10years of MERIS observations. Remote Sens. Environ. 158, 441–452.
Park, K., Park, J.-E., Lee, M.-S., Kang, C.-K., 2012. Comparison of composite methods of satellite chlorophyll-a concentration data in the East Sea. Korean J. Remote Sens. 28, 635–651.
Perkins, T., Adler-Golden, S., Matthew, M.W., Berk, A., Bernstein, L.S., Lee, J., et al., 2012. Speed and accuracy improvements in FLAASH atmospheric correction of hyperspectral imagery. Opt. Eng. 51, 111707-1.
Pietrzak, J.D., de Boer, G.J., Eleveld, M.A., 2011. Mechanisms controlling the intra-annual mesoscale variability of SST and SPM in the southern North Sea. Cont. Shelf Res. 31, 594–610.
Pleskachevsky, A., Gayer, G., Horstmann, J., Rosenthal, W., 2005. Synergy of satellite remote sensing and numerical modeling for monitoring of suspended particulate matter. Ocean Dyn. 55, 2–9.
Przyborska, A., Muzyka, M., Andrzejewski, J., Jakacki, J., Rak, D., 2020. The spreading of suspended matter formed during construction works of offshore wind farms. 22nd EGU General Assembly, Vienna, p. 13845.
Python, 2022. Datetime: Basic Date and Time Types.
Rijnsburger, S., Flores, R.P., Pietrzak, J.D., Horner-Devine, A.R., Souza, A.J., 2018. The influence of tide and wind on the propagation of fronts in a shallow river plume. J. Geophys. Res. Oceans 123, 5426–5442.
Sainani, K.L., 2016. The value of scatter plots. PM&R 8, 1213–1217.
Slavik, K., Lemmen, C., Zhang, W., Kerimoglu, O., Klingbeil, K., Wirtz, K.W., 2019. The large-scale impact of offshore wind farm structures on pelagic primary productivity in the southern North Sea. Hydrobiologia 845, 35–53.
Spiegelhalter, D.J., Best, N.G., Carlin, B.P., Van Der Linde, A., 2002. Bayesian measures of model complexity and fit. J. R. Stat. Soc. Ser. B (Stat. Methodol.) 64, 583–639.
Stanev, E.V., Dobrynin, M., Pleskachevsky, A., Grayek, S., Günther, H., 2009. Bed shear stress in the southern North Sea as an important driver for suspended sediment dynamics. Ocean Dyn. 59, 183–194.
Suijlen, J.M., Duin, R.N.M., 2002. Atlas of near-surface total suspended matter concentrations in the Dutch coastal zone of the North Sea. Rapportnr.: 2002.059.
Svane, I.B., Petersen, J.K., 2001. On the problems of epibioses, fouling and artificial reefs, a review. Mar. Ecol. 22, 169–188.
Swart, R.J., Coppens, C., Gordijn, H., Piek, M., Ruyssenaars, P., Schrander, J.J., et al., 2009. Europe's Onshore and Offshore Wind Energy Potential: An Assessment of Environmental and Economic Constraints. European Environment Agency, Copenhagen.
Underwood, A.J., 1992. Beyond BACI: the detection of environmental impacts on populations in the real, but variable, world. J. Exp. Mar. Biol. Ecol. 161, 145–178.
UNFCCC, 2015. Historic Paris Agreement on Climate Change, 195 Nations Set Path to Keep Temperature Rise Well Below 2 Degrees Celsius.
Unidata, 2022. netCDF4: Introduction.
Van der Molen, J., Ruardij, P., Greenwood, N., 2017. A 3D SPM model for biogeochemical modelling, with application to the northwest European continental shelf. J. Sea Res. 127, 63–81.
Van der Molen, J., Van Leeuwen, S.M., Govers, L.L., Van der Heide, T., Olff, H., 2021. Potential micro-plastics dispersal and accumulation in the North Sea, with application to the MSC Zoe incident. Front. Mar. Sci. 195.
van der Spek, A., van der Werf, J., Oost, A., Vermaas, T., Grasmeijer, B., Schrijvershof, R., 2022. The lower shoreface of the Dutch coast – an overview. Ocean Coast. Manag. 230, 106367.
Vanhellemont, Q., 2019a. Adaptation of the dark spectrum fitting atmospheric correction for aquatic applications of the Landsat and Sentinel-2 archives. Remote Sens. Environ. 225, 175–192.
Vanhellemont, Q., Ruddick, K., 2014. Turbid wakes associated with offshore wind turbines observed with Landsat 8. Remote Sens. Environ. 145, 105–115.
Vanhellemont, Q., Ruddick, K., 2018. Atmospheric correction of metre-scale optical satellite data for inland and coastal water applications. Remote Sens. Environ. 216, 586–597.
Wang, M., 2007. Remote sensing of the ocean contributions from ultraviolet to near-infrared using the shortwave infrared bands: simulations. Appl. Opt. 46, 1535–1547.
Waskom, M.L., 2021. Seaborn: statistical data visualization. J. Open Source Softw. 6, 3021.
Waters, T.F., 1995. Sediment in Streams: Sources, Biological Effects, and Control.
Wiser, R., Yang, Z., Hand, M., Hohmeyer, O., Infield, D., Jensen, P.H., et al., 2011. Wind energy. IPCC Special Report on Renewable Energy Sources and Climate Change Mitigation, pp. 535–608.
WWF-Norway, 2014. Environmental impacts of Offshore Wind Poer Production in the North Sea. A Literature Overview. WWF-World Wide Fund For Nature (Formerly World Wildlife Fund), Oslo, Norway, p. 46.
Zijl, F., Laan, S.C., Emmanouil, A., van Kessel, T., van Zelst, V.T.M., Vilmin, L.M., et al., 2021. Potential Ecosystem Effects of Large Upscaling of Offshore Wind in the North Sea: Bottom-up Approach. Deltares, p. 96.